npg

Bak apoptotic pores involve a flexible C-terminal region and juxtaposition of the C-terminal transmembrane domains

S Iyer[1,2], F Bell[1], D Westphal[1,2], K Anwari[1,2], J Gulbis[1,2], BJ Smith[3], G Dewson[1,2] and RM Kluck*[1,2]

Bak and Bax mediate apoptotic cell death by oligomerizing and forming a pore in the mitochondrial outer membrane. Both proteins anchor to the outer membrane via a C-terminal transmembrane domain, although its topology within the apoptotic pore is not known. Cysteine-scanning mutagenesis and hydrophilic labeling confirmed that in healthy mitochondria the Bak α9 segment traverses the outer membrane, with 11 central residues shielded from labeling. After pore formation those residues remained shielded, indicating that α9 does not line a pore. Bak (and Bax) activation allowed linkage of α9 to neighboring α9 segments, identifying an α9:α9 interface in Bak (and Bax) oligomers. Although the linkage pattern along α9 indicated a preferred packing surface, there was no evidence of a dimerization motif. Rather, the interface was invoked in part by Bak conformation change and in part by BH3:groove dimerization. The α9:α9 interaction may constitute a secondary interface in Bak oligomers, as it could link BH3:groove dimers to high-order oligomers. Moreover, as high-order oligomers were generated when α9:α9 linkage in the membrane was combined with α6:α6 linkage on the membrane surface, the α6-α9 region in oligomerized Bak is flexible. These findings provide the first view of Bak carboxy terminus (C terminus) membrane topology within the apoptotic pore.

Cell Death and Differentiation (2015) 22, 1665–1675; doi:10.1038/cdd.2015.15; published online 6 March 2015

Mitochondrial permeabilization during apoptosis is regulated by the Bcl-2 family of proteins.[1–3] Although the Bcl-2 homology 3 (BH3)-only members such as Bid and Bim trigger apoptosis by binding to other family members, the prosurvival members block apoptosis by sequestering their pro-apoptotic relatives. Two remaining members, Bak and Bax, form the apoptotic pore within the mitochondrial outer membrane (MOM).

Bak and Bax are globular proteins comprising nine α-helices.[4,5] They are activated by BH3-only proteins binding to the α2–α5 surface groove,[6–12] or for Bax, to the α1/α6 'rear pocket'.[13] Binding triggers dissociation of the latch domain (α6–α8) from the core domain (α2–α5), together with exposure of N-terminal epitopes and the BH3 domain.[6,7,14–16] The exposed BH3 domain then binds to the hydrophobic groove in another Bak or Bax molecule to generate symmetric homodimers.[6,7,14,17,18] In addition to dimerizing, parts of activated Bak and Bax associate with the lipid bilayer.[19] In Bax, the α5 and α6 helices may insert into the MOM,[20] although recent studies indicate that they lie in-plane on the membrane surface, with the hydrophobic α5 sandwiched between the membrane and a BH3:groove dimer interface.[7,21–23] The dimers can be linked via cysteine residues placed in α6,[18,24,25] and more recently via cysteine residues in either α3 or α5,[6,21] allowing detection of the higher-order oligomers associated with pore formation.[26,27] However, whether these interactions are required for high-order oligomers and pore formation remains unclear.

Like most Bcl-2 members, Bak and Bax are targeted to the MOM via a hydrophobic C-terminal region. The C terminus targets Bak to the MOM in healthy cells,[28] whereas the Bax C terminus is either exposed[29] or sequestered within the hydrophobic groove until apoptotic signals trigger Bax translocation.[5,30,31] The hydrophobic stretch is important, as substituting polar or charged residues decreased targeting of Bak and Bax.[10,32] Mitochondrial targeting is also controlled by basic residues at the far C termini,[32–34] and by interaction with VDAC2[35,36] via the Bak and Bax C termini.[37,38] Retro-translocation of Bak and Bax was also altered by swapping the C termini.[39]

The membrane topology of the Bak and Bax C termini before and after apoptosis has not been examined directly, due in part to difficulty in reconstituting oligomers of full-length Bak in artificial membranes. Nor is it known whether the C termini contribute to pore formation by promoting oligomerization or disturbing the membrane. To address these questions synthetic peptides based on the Bak and Bax C termini have been studied in model membranes. The peptides adopt a predominantly α-helical secondary structure,[40–43] with orientation affected by lipid composition.[42,44,45] The peptides could also permeabilize lipid vesicles,[41,43,46,47] suggesting that the

[1]The Walter and Eliza Hall Institute of Medical Research, Parkville, Victoria 3050, Australia; [2]Department of Medical Biology, The University of Melbourne, Parkville, Victoria 3010, Australia and [3]Department of Chemistry and Physics, La Trobe Institute for Molecular Sciences, La Trobe University, Melbourne, Victoria 3086, Australia
*Corresponding author: R Kluck, The Walter and Eliza Hall Institute of Medical Research, Parkville, Victoria 3050, Australia. Tel: +61 3 9345 2487; Fax: +61 3 9347 0852;
E-mail: kluck@wehi.edu.au

Abbreviations: BH3, Bcl-2 homology 3; BMOE, 1,6-bis-maleimidoethane; C terminus, carboxy terminus; CuPhe, copper(II)(1,10-phenanthroline)$_3$; FRET, Förster resonance energy transfer; GFP, green fluorescent protein; IASD, 4-acetamido-4′-((iodoacetyl)amino)stilbene-2,2′-disulfonic acid; IEF, isoelectric focusing; IRES, internal ribosome entry site; MEFs, mouse embryonic fibroblasts; MOA, monoamine oxidase A; MOM, mitochondrial outer membrane; SDS-PAGE, SDS-polyacrylamide electrophoresis; S/N, supernatant; tBid, truncated Bid; wt, wild type; TMD, transmembrane domain.

C termini in full-length Bak and Bax may contribute to pore formation.

Here we examined the membrane topology of the C termini within full-length Bak and Bax in the MOM, both before and after apoptotic pore formation. After pore formation the α9 helices of Bak (and of Bax) became juxtaposed but did not line the surface of a pore. The α9:α9 interaction occurred after Bak activation and conformation change, but was promoted by formation of BH3:groove dimers. Combining linkage at more than one interface indicated that the Bak α9:α9 interface can link BH3:groove dimers to high-order oligomers, and moreover, that the α6–α9 region is flexible in oligomerized Bak.

Results

Cysteine substitutions in α9 can hinder Bak insertion into the MOM, but only prior to Bak activation. To explore the membrane topology of the Bak C terminus, cysteine residues were introduced throughout the predicted α9 helix (I188–V205) (Figures 1a and b) using cysteine-null human Bak (C14S/C166S) as the template. When stably expressed in $Bax^{-/-}Bak^{-/-}$ MEFs,[14] each variant expressed at levels similar to that of wild-type (wt) Bak, and retained pro-apoptotic function (Supplementary Figures S1a and b), indicating that the substitutions were well tolerated. Substitution at certain positions reduced Bak targeting and insertion, as some Bak was evident in the cytosol (Figure 1b, lane 1) or was peripherally attached after carbonate extraction (Figure 1b, lane 2). Notably, however, all peripherally attached Bak became carbonate resistant following incubation of mitochondria with truncated Bid (tBid) (Figure 1b, lane 4). Thus, Bak activation enhances α9 membrane insertion, as observed for a semi-cytosolic Bak mutant[33] and for Bax.[48]

Bak α9 traverses the MOM but does not line a pore following apoptosis. To identify α9 residues buried in the hydrophobic interior of the MOM, cysteine variants were labeled with the membrane-impermeable sulfhydryl reagent 4-acetamido-4′-((iodoacetyl)amino)stilbene-2,2′-disulfonic acid (IASD).[20,23,49] The two negative charges on IASD prevent its entry into hydrophobic regions, including membranes, protein interior and protein interfaces.[23] IASD efficiently labeled cysteine residues on the cytoplasmic side of the MOM (Figures 2a, e and g; G186C). IASD also strongly labeled cysteine placed at the far C terminus (Figure 2a, BakGGCK), probably by passing through channels[20,50] such as VDAC, which allows passage of metabolites up to 4000 Da.[51] Quantification of IASD labeling before and after tBid is shown in Figure 2b.

In the middle of α9, an 11-residue stretch (V191C-G201C) displayed limited IASD labeling (Figures 2a and b), indicating burial in the MOM. Some of these residues were more labeled prior to tBid, consistent with a population having been peripherally attached (see Figure 1b) but inserting upon activation. At the proximal end of α9, four residues (G186C–L189C) were fully labeled before and after tBid. The next residue (N190C) was ~50% labeled, placing it at the threshold of IASD accessibility. We expected to see a reciprocal gradient of IASD labeling at the α9 carboxy end as the helix exits the
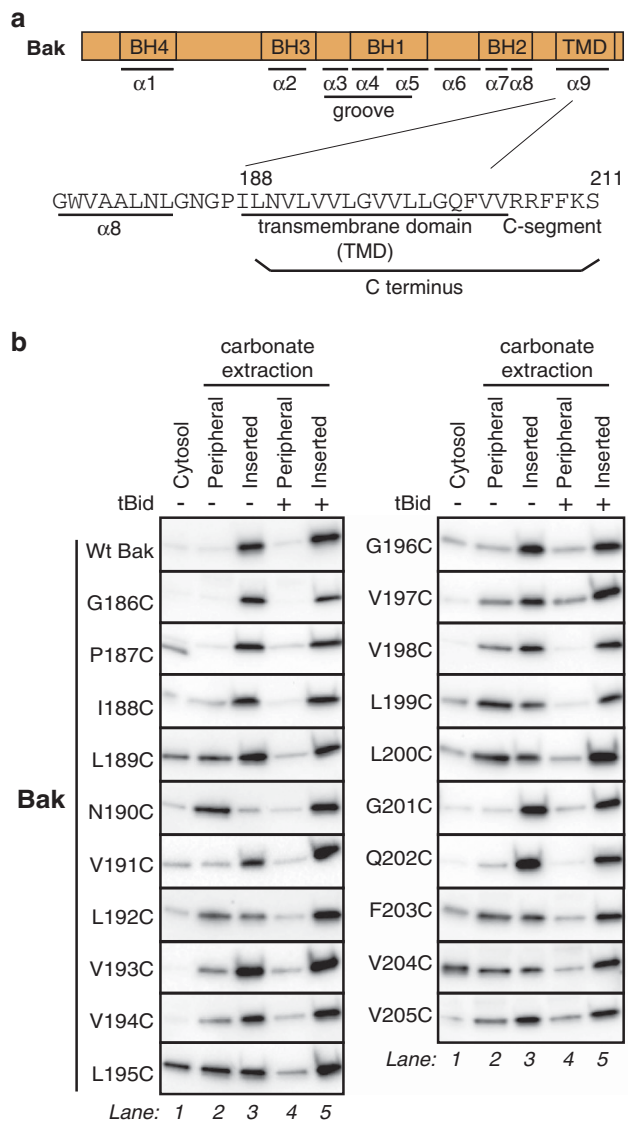

Figure 1 Cysteine substitutions in α9 can hinder Bak mitochondrial insertion, but only prior to apoptosis. (**a**) The Bak C terminus comprises a hydrophobic transmembrane domain and a basic C-segment. Positions of the four Bcl-2 homology (BH) domains and C-terminal transmembrane domain in Bak are shown, as is part of the human Bak sequence. (**b**) Bak mitochondrial localization is decreased by cysteine substitutions in α9, but membrane insertion is complete after activation by tBid. Untreated cells were fractionated into cytosol and membrane fractions, and the membrane fractions then extracted with sodium carbonate to detect peripherally attached and membrane-inserted populations. Where indicated, membrane fractions were pre-treated with tBid to activate Bak. Data are representative of three independent experiments

MOM and enters the intermembrane space. However, four consecutive residues (Q202C–V205C) showed ~50% labeling before tBid (Figure 2a), suggesting these residues may be non-helical. On the basis of the cysteine labeling data, Figure 2c illustrates the possible membrane topology of Bak α9 prior to activation.

After Bak activation and pore formation, four residues (Q202C–V205C) at the α9 carboxy terminus showed greater labeling (Figures 2a and b), suggesting some relationship of
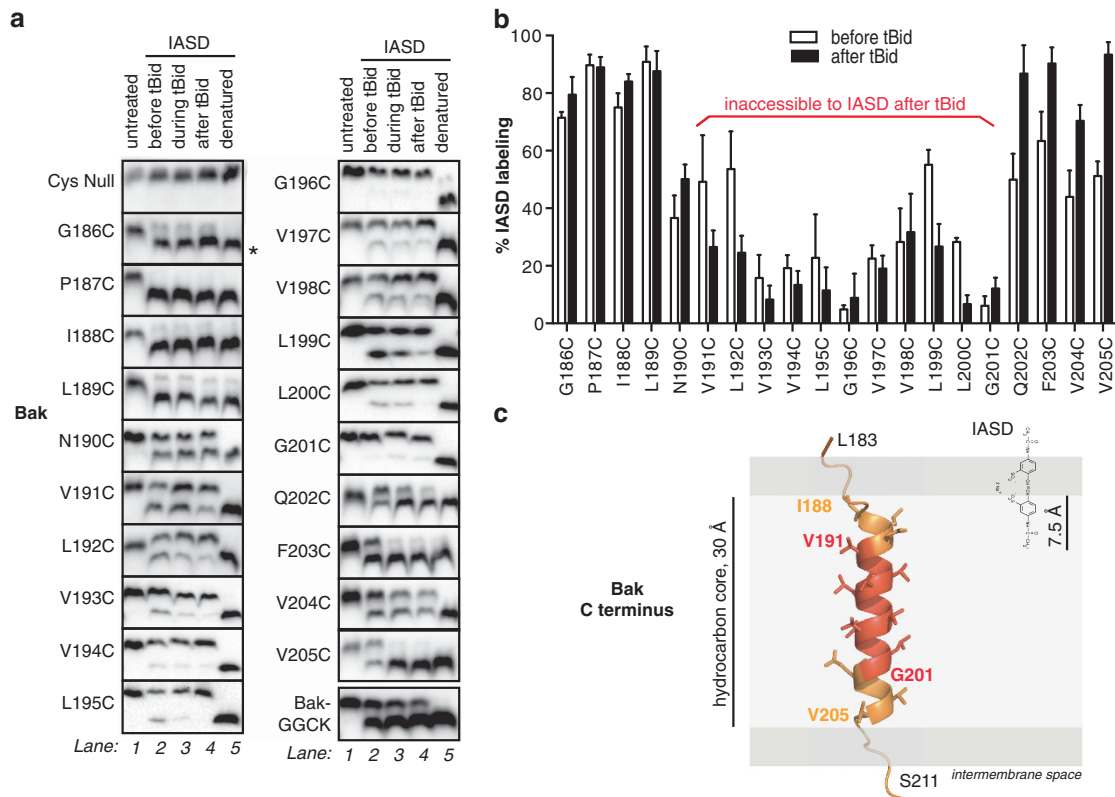
Figure 2 Bak α9 traverses the MOM but does not line a pore following apoptosis. (**a**) Cysteine accessibility approach reveals the transmembrane nature of Bak α9. Membrane fractions from MEFs expressing the indicated Bak variants were incubated with tBid and IASD as follows. In lane 1, mitochondria-enriched membranes were untreated. In lanes 2 and 4, membranes were incubated in the absence or presence of tBid, and then with IASD. In lane 3, IASD was present during the tBid incubation to detect both transient and persistent exposure. In lane 5, membranes were solubilized with detergent prior to treatment with IASD to obtain complete labeling. Samples were run on one-dimensional isoelectric focusing gels and immunoblotted for Bak. Asterisk (*) denotes IASD-labeled Bak. BakGGCK has four residues (GGCK) added to the carboxy terminus (see Figure 4). Data are representative of three independent experiments. (**b**) Quantified IASD labeling of Bak α9 before and after tBid. Data are mean ± S.D. of three independent experiments. (**c**) Membrane topology of the Bak C terminus prior to Bak activation. As the Bak C terminus is not present in the X-ray structure of Bak,[4] the Jpred-3 structure prediction server[69] was used to predict which residues are likely to adopt an α-helical geometry (I188–V205). The structure of α9 was modeled using the SyByL software.[70] The α-helix was then positioned in the membrane assuming that IASD is able to label cysteine side-chains 7.5 Å into the hydrocarbon core due to the distance between the charged (hydrophilic) and reactive (iodoacetamide) groups of IASD.[71] Assuming 1.5 Å per residue for the α-helical conformation, the 11 IASD-inaccessible residues (red) can span 15 Å in the center of the hydrocarbon bilayer. We cannot rule out that α9 adopts a 3₁₀-helix configuration;[72] in this case, the TMD would extend ~ 3 Å longer than an α-helix, changing the side-chain orientation on the α9 carboxy terminus, potentially beyond the confines of the membrane. The width of the hydrocarbon bilayer is represented as 30 Å[42]

α9 to pore formation. As Supplementary Figure S2 illustrates, α9 may become shorter or IASD may penetrate further into the MOM inner leaflet. The labeling is not consistent with α9 positioning deeper in the membrane, or membrane thinning. Notably, as central residues of α9 did not label along one edge after tBid treatment, α9 does not line the Bak apoptotic pore.

An α9:α9 interface forms in oligomerized Bak and exhibits a distinctive cysteine linkage pattern. To test the proximity of α9 helices before and/or after Bak becomes activated, we used cysteine linkage (Figure 3a). Assuming the cysteine in each Bak molecule would be co-planar within the MOM, if they are also adjacent to each other (~4 Å between β-carbons) they may form a disulfide bond after addition of the oxidant copper(II)(1,10-phenanthroline)₃ (CuPhe).[52] To link cysteine residues further apart, the chemical crosslinker bis-maleimidoethane (BMOE, spacer arm 8 Å) was used.

Prior to tBid treatment, there was no linkage of α9 cysteines using either CuPhe or BMOE (Figure 3a), consistent with nonactivated Bak being distributed across the MOM surface. Some linkage to other MOM proteins was evident upon CuPhe treatment, particularly for V205C, and less so for G186C and P187C (Figure 3a). Furthermore, different MOM proteins became linked to residues at either end of α9, consistent with α9 spanning the MOM.

After tBid treatment, linkage of several α9 residues was evident (Figure 3a), showing for the first time that the α9 helices become juxtaposed during Bak oligomerization and pore formation. The degree of linkage by CuPhe varied for cysteine residues positioned throughout α9 (Figure 3a), as illustrated on a model of the Bak C terminus (Figure 3b). A similar linkage pattern was induced by BMOE (Figure 3a), with some differences attributable to the greater length of the BMOE linker (8 Å) or to the ability of CuPhe to capture dynamic interactions.[52]
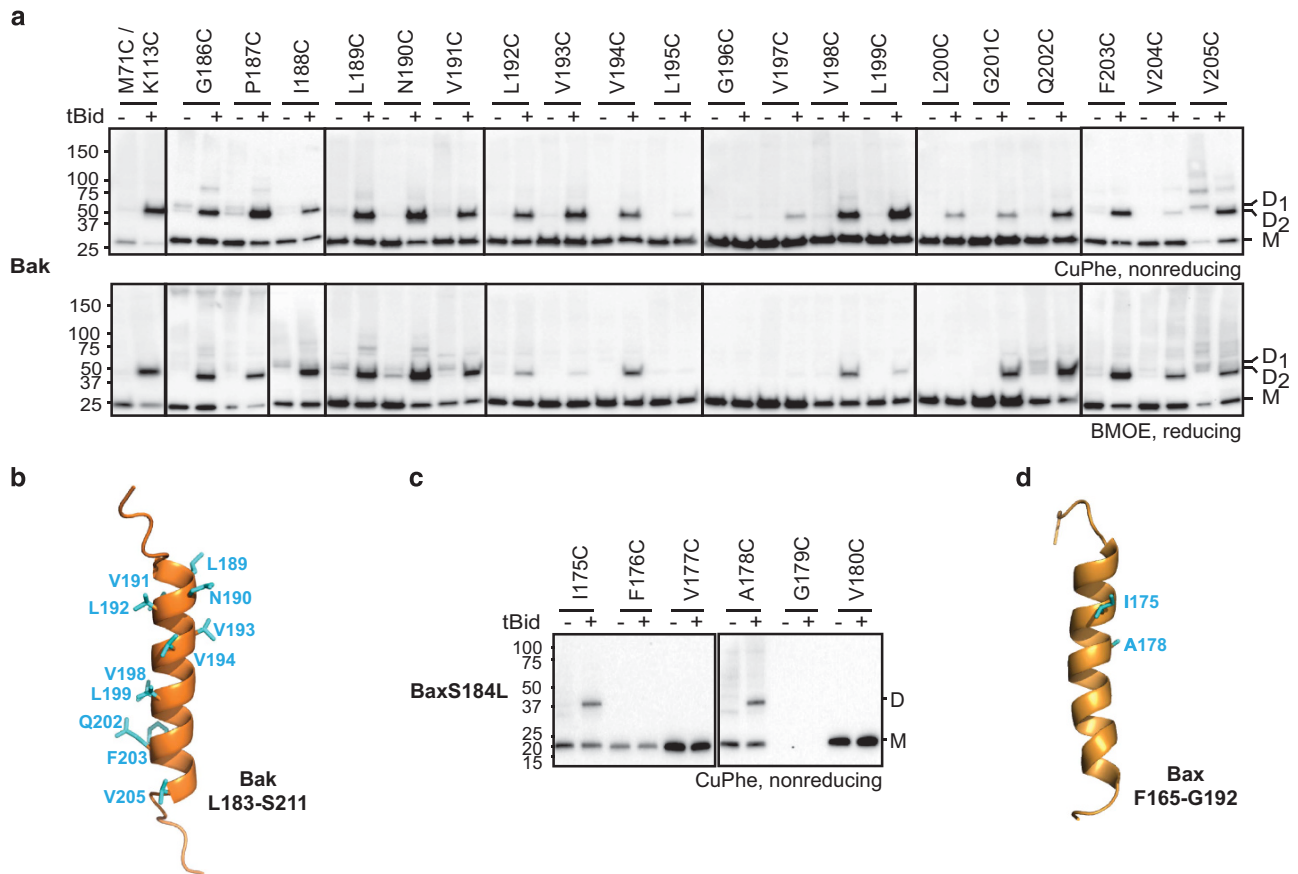
Figure 3 The Bak and Bax *α*9 helices can be linked following an apoptotic stimulus. (**a**) Intermolecular *α*9:*α*9 linkage can be captured after Bak becomes activated. Membrane fractions from *Bak*^{−/−}*Bax*^{−/−} MEFs expressing the indicated Bak cysteine variants were incubated without or with tBid prior to treatment with the oxidant CuPhe (upper panel) or the crosslinker BMOE (lower panel). Unlinked Bak (M, monomer) or linked Bak (D, dimer) was detected following SDS-PAGE (nonreducing for CuPhe) and immunoblotting for Bak. To compare with linkage at the BH3:groove interface, the M71C/K113C variant is included in lanes 1 and 2. (The BH3:groove-linked dimers (D₁) migrate slower than dimers linked at the *α*9:*α*9 interface (D₂), and the M71C/K113C samples were run on the same gels as the L189C, N190C and V191C samples.) Data are representative of at least three independent experiments. (**b**) Linkage pattern at the *α*9:*α*9 interface in activated Bak. Cartoon of the Bak C terminus from Figure 2c highlighting residues (cyan) that can link to the equivalent residue in a neighboring activated Bak molecule. (**c**) Intermolecular *α*9:*α*9 linkage can be captured after BaxS184L becomes activated. Membrane fractions from *Bak*^{−/−}*Bax*^{−/−} MEFs expressing the indicated BaxS184L cysteine variants were incubated with tBid and CuPhe as in **a**. Data are representative of at least three independent experiments. (**d**) Linkage pattern at the *α*9:*α*9 interface in activated BaxS184L. Cartoon of the Bax C terminus (1F16)[5] highlighting residues (cyan) that can link to the equivalent residue in a neighboring activated BaxS184L molecule

Activated Bax also exhibits *α*9:*α*9 linkage with a distinctive cysteine linkage pattern. To test whether an *α*9:*α*9 interface also occurs in Bax after it becomes oligomerized, a single cysteine was placed at six positions in *α*9 of a mitochondrial form of Bax, S184L[53] (Figure 3c). Each variant was able to mediate apoptosis after etoposide, even the G179C variant which, as observed previously,[20] expressed at very low levels (Supplementary Figure S1c). When membrane fractions were incubated with tBid, CuPhe was able to link *α*9 at two positions (I175C and *α*178C)(Figures 3c and d). A similar linkage pattern was detectable in wt Bax in apoptotic cells (Supplementary Figure S3). Thus, Bak oligomers and Bax oligomers both contain an *α*9:*α*9 interface, and both display a distinctive linkage pattern.

Extensions to the C-segment show greater linkage after Bak and Bax are activated. We also monitored C-terminal proximity as viewed from the intermembrane space by adding

a cysteine residue to the C-segment (Figure 4a). To encourage the extended C-segment to cross the membrane as normal, a basic residue (Lys) was incorporated as the terminal residue. This approach was successful, as the extensions did not impair Bak or Bax expression or function (Supplementary Figures S1d and e).

Prior to tBid, only minor linkage between the Bak extensions was evident despite the flexible linker (GGSGG) and cysteine being 11 residues from *α*9 in the GGSGGCK variant (Figure 4b). The absence of linkage to other Bak molecules indicates that in healthy mitochondria the Bak *α*9 helices may not approach within 20–30 Å, even transiently. After tBid, each Bak extension could be linked by CuPhe (Figure 4b). Extensions to Bax also showed strong linkage in membrane fractions after etoposide-induced apoptosis (Figure 4c).

An *α*9:*α*9 association occurs in the absence of BH3: groove dimerization. To test whether the *α*9:*α*9 interface in

a


```
                    Transmembrane domain    C-segment
        183
Bak        LGNGPILNVLVVLGVVLLGQFVVRRFFFKS 211
BakCK      LGNGPILNVLVVLGVVLLGQFVVRRFFFKSCK
BakGGCK    LGNGPILNVLVVLGVVLLGQFVVRRFFFKSGGCK
BakGGSGGCK LGNGPILNVLVVLGVVLLGQFVVRRFFFKSGGSGGCK

         165
Bax         FGTPTWQTVTIFVAGVLTASLTIWKKMG 192
BaxGGCK     FGTPTWQTVTIFVAGVLTASLTIWKKMGGGCK
BaxGGSCK    FGTPTWQTVTIFVAGVLTASLTIWKKMGGGSCK
```
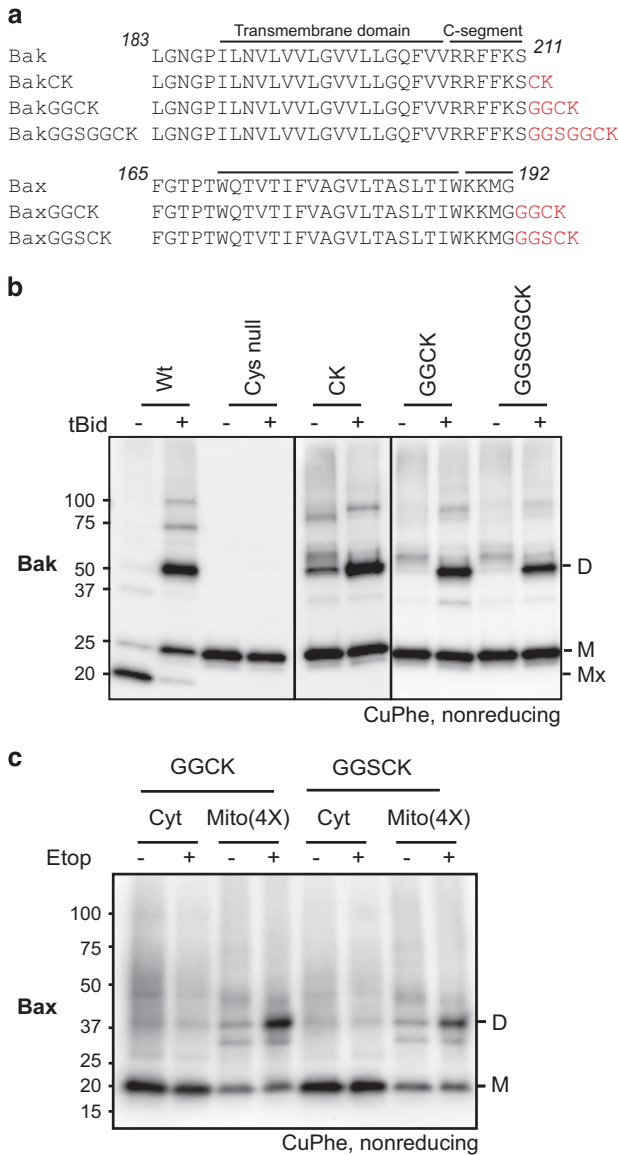
b

c

Figure 4 Extensions to the C-segments of Bak and Bax can be linked only after Bak and Bax are activated. (**a**) Extensions to the C-segments. Extra residues (red) added to Bak and Bax contain cysteine to monitor linkage, glycine to provide flexibility, and lysine to encourage targeting and insertion into the MOM. (**b**) C-segment extensions to Bak can be linked after but not before apoptosis. Membrane fractions from $Bak^{-/-}Bax^{-/-}$ MEFs expressing the indicated C-segment variants were incubated without or with tBid prior to treatment with CuPhe. Samples were analyzed as in Figure 3a. Mx indicates an intramolecular cysteine disulfide bond (C14:C166) in nonactivated wt Bak. Note that in the absence of tBid, some linkage to other mitochondrial proteins was evident (Figure 4b), as observed for the nearby V205C (Figure 3a). Note also that some degree of linkage routinely occurred in the CK variant, suggesting that this variant may be arranged a little differently to other variants prior to its activation. Data are representative of at least three independent experiments. (**c**) C-segment extensions to Bax can be linked after but not before apoptosis. $Bak^{-/-}Bax^{-/-}$ MEFs expressing the indicated C-segment variants were cultured in the presence of etoposide, and the cytosol (Cyt) and membrane (Mito) fractions incubated with CuPhe. The cytosol and fourfold-enriched membrane fractions were analyzed as in Figure 3a, but immunoblotted for Bax. Data are representative of at least three independent experiments

activated Bak occurs before or after BH3:groove dimer formation, we blocked the BH3:groove interface and asked whether $a9:a9$ linkage was also blocked. In one approach, membrane fractions were incubated with tBid in the presence of the 4B5 antibody that can capture the transiently exposed Bak BH3 domain.[14,24] As expected, 4B5 blocked cytochrome c release mediated by each Bak variant, whereas the control antibody did not (Figure 5). 4B5 also inhibited linkage at the BH3:groove and $a6:a6$ interfaces (Figure 5), as seen previously.[14,24] However, linkage at $a9:a9$ was largely unaffected (Figure 5, top), indicating that the $a9$ helices can come into proximity after Bak has undergone conformation change but before BH3:groove dimerization.

In a second approach, the BH3:groove interface was inhibited by mutating the Bak BH3 domain (I81T) or groove (F93S). As expected from our previous work,[14] these variants were deficient in mediating apoptosis (Supplementary Figure S1f). Moreover, when membrane fractions were incubated with tBid, linkage at the BH3:groove and $a6:a6$ interfaces was decreased by ~50% (Supplementary Figure S4). Linkage at $a9:a9$ was also partly inhibited, suggesting that BH3:groove dimerization can enhance the $a9:a9$ interface. Although neither approach completely blocked BH3:groove linkage, together they indicate that proximity of the $a9$ helices can occur after Bak activation, but may be promoted by BH3:groove dimerization.

An alternative C terminus in Bak can also be linked after oligomerization. To test the role of the Bak C-terminal sequence in driving the $a9:a9$ interface, the Bak C terminus was swapped with the C terminus of other tail-anchored proteins (Figure 6a). The swaps were positioned after P187, as placing the Bax C terminus at this position had successfully maintained Bak localization and apoptotic function.[33] Swaps were generated from Bcl-2 and mono-amine oxidase A (MOA), as they normally locate to the MOM,[54,55] with BakBcl2 containing two extra residues (RK) used to enhance mitochondrial targeting.[55] Swaps were also generated from BNIP3 and glycophorin A, as their trans-membrane domains (TMDs) contain known dimerization motifs (e.g., GxxxG), and the two proteins localize to the MOM and cell membrane, respectively.[56,57] We also generated a glycophorin-like motif (GxxxG) in Bak $a9$ simply by reversing two residues to generate ^{196}GVVLG^{201}. Finally, a C-terminal swap from Fis1 was examined, as the Fis1 C terminus could target Bak to mitochondria.[37] All chimeras contained the CK extension described in Figure 4. Thus, these chimeras had the potential to identify a role for TMD dimerization domains in promoting Bak oligomerization and pore formation. In addition, we could identify chimeras that might mediate apoptosis without forming an $a9:a9$ interface.

Four chimeras (BakBcl2, BakBNIP3, BakGphA, BakMOA) showed low expression (Figure 6b) and/or poor localization to mitochondria (Figure 6c), highlighting the role of the C terminus in Bak mitochondrial localization and stabilization. The dimerization domains in BakBNIP3 and BakGpHA were functional, as indicated by linked dimers in the membrane fraction even before treatment with tBid (Figure 6d), although the very low protein levels precluded any conclusion on whether the dimerized C termini in those two variants might
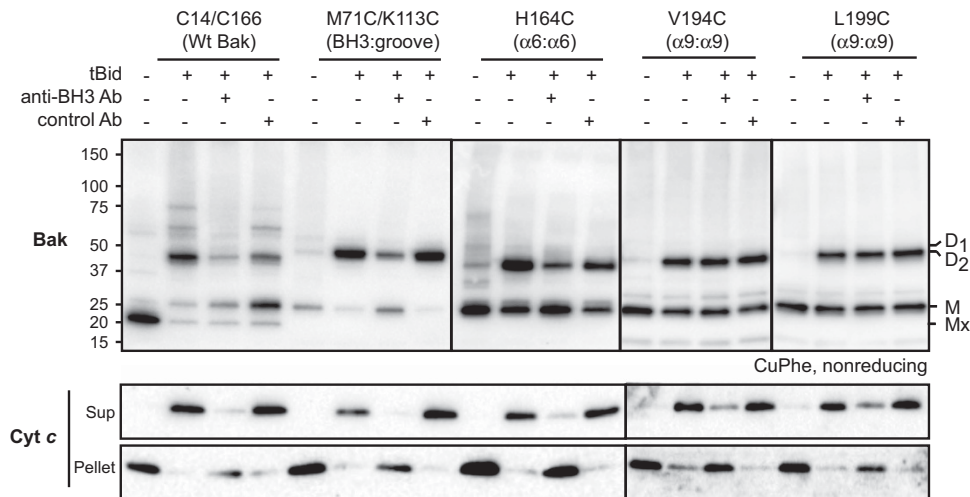
Figure 5 The Bak α9:α9 interface is not impeded when an antibody inhibits the BH3:groove interface. Membrane fractions from $Bak^{-/-}Bax^{-/-}$ MEFs expressing the indicated cysteine variants were incubated without or with tBid. Where indicated, an anti-BH3 (4B5) or control antibody to the Bak N terminus (8F8)[24] was also present (at 5 μg per 50 μl sample) during the incubation. Aliquots were assessed for cysteine linkage by CuPhe as in Figure 3a, or for cytochrome c release. Mx indicates an intramolecular cysteine disulfide bond (C14:C166) in nonactivated wt Bak. Data are representative of at least three independent experiments

promote pore formation (Figures 6b–d). Lack of cytochrome c release by BakBcl2 and BakMOA (Figure 6d) may also be explained by low protein levels in the membrane fraction (Figure 6c) or by targeting to non-mitochondrial membranes. Unfortunately, the GxxxG motif in Bak α9 failed to dimerize the C termini before tBid (Figure 6d). In summary, these five Bak variants provided little insight into whether an α9 dimerization domain might help drive pore formation.

Another chimera, BakFis1, did support pore formation as cells expressing BakFis1 died efficiently after etoposide treatment (Figure 6b), and mitochondria expressing BakFis1 released cytochrome c in response to tBid (Figure 6d). Notably, the C-segment in BakFis1 could also be linked after tBid treatment (Figure 6d). Thus, the C terminus from Fis1 can substitute for that of Bak to allow both pore formation and a C-terminal interface.

An α9:α9 interface is distinct from the BH3:groove and α6:α6 interfaces. We next sought to understand the topology of the α9:α9 interface in relation to that of the BH3:groove interface. Previously, combining linkage at the Bak BH3:groove and α6:α6 interfaces generated higher-order oligomers, indicating the two interfaces are distinct and complementary.[24] We thus generated Bak variants with cysteines positioned at the α9:α9 interface and at interfaces on either side of the MOM: each retained pro-apoptotic function (Supplementary Figure S1g). When cysteines in the BH3:groove and α9:α9 interfaces were combined, higher-order complexes were apparent, and the complexes were similar to those generated by α6:α6 linkage (MK/H164C) (Figure 7a). Thus, as argued for the α6:α6 interface,[24] the α9:α9 interface is distinct from the BH3:groove interface, and can link the BH3:groove dimers (D_1) to higher-order oligomers.

Combining linkage at the α6:α6 and α9:α9 interfaces also generated higher-order oligomers (Figure 7b), as did combining linkage at the C-segment (GGCK) with linkage at the BH3: groove or α6:α6 interfaces on the cytosolic side of the MOM, or with α9:α9 within the MOM (Figure 7c). These findings indicate

that in oligomerized Bak, the region encompassing α6 to the C-segment is flexible rather than constrained by tight protein–protein interactions, as illustrated in Figure 7d.

Discussion

We examined the membrane topology of the Bak C-terminal latch (α6–α8) and TMD (α9) to help define the topology of Bak dimers and high-order oligomers in apoptotic pores. In addition, we examined whether the α9 helix (or the α9:α9 interface) might be necessary for the step of pore formation, as α9 appears to be the only region that traverses the MOM before and after pore formation,[21–23] and α9 peptides have been proposed to be membranolytic with antitumor activity.[43,58] Thus, understanding α9 membrane topology may reveal novel insight for cancer therapy.

Bak α9 as a transmembrane domain. Cysteine labeling and linkage data were consistent with the Bak TMD being predominantly helical, and with that helix traversing the MOM. For example, 11 central residues were poorly labeled by IASD, consistent with the distance covered by a single span of the mitochondrial membrane. Moreover, residues at either end could link to other proteins present in the mitochondrial preparations. Structures of many MOM tail-anchored proteins including Bax, MOA, glycophorin A and BNIP3 show helical TMDs.[5,57,59,60] The Bak TMD may, however, be non-helical at the carboxy terminus, as partial IASD labeling of four sequential residues is unlikely for a helical TMD. In model membranes, peptides based on the Bak and Bax C termini showed mixtures of secondary structure,[42,44] and the Fis1 C terminus was disordered in NMR studies.[61] Thus, helicity of the TMD may not be necessary for any aspect of Bak function.

Our findings confirm the role of α9 in targeting Bak to mitochondria, as a decrease in α9 hydrophobicity produced by cysteine substitution caused a small decrease in Bak targeting and insertion. After Bak was activated, the peripheral α9
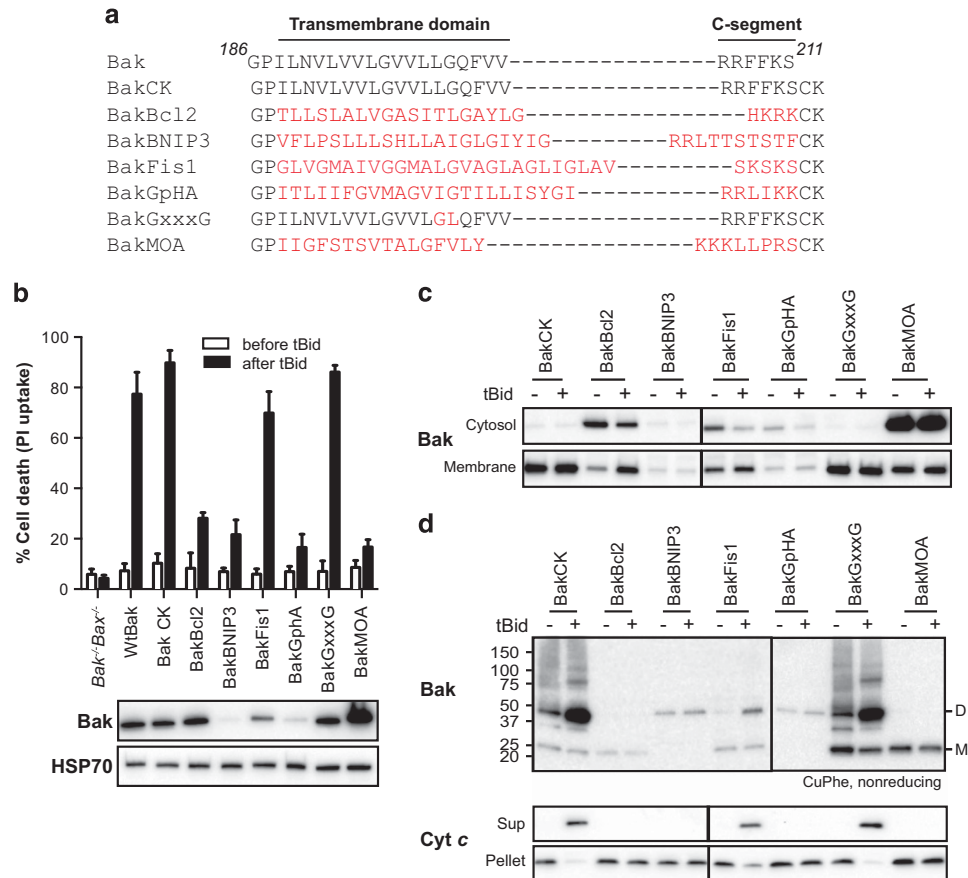
Figure 6 An alternative C terminus in Bak can also be linked after oligomerization. (**a**) Sequences of Bak C-terminal chimeras. The whole C terminus (186-211) of Bak was replaced with that of Bcl-2, BNIP3, Fis1, glycophorin A (GpHA) or monoamine oxidase A (MOA) (highlighted in red). To generate a glycophorin-like dimerization motif (GxxxG) in Bak α9, two residues (LG) were reversed to obtain ^{196}GVVLG^{201}. Cysteine and lysine were added to monitor linkage and to encourage targeting and insertion into the MOM, as in Figure 4. (**b**) Bak containing the Fis1 C terminus retains stability and function. $Bak^{-/-}Bax^{-/-}$ MEFs expressing the indicated Bak chimeras were treated with etoposide and assessed for cell death (top panel). Data are mean ± S.D. from three independent experiments. Total cell lysates from untreated cells were immunoblotted for Bak, and for HSP70 as a loading control (bottom panels). (**c**) BakFis1 is semi-cytosolic but can translocate to mitochondria after tBid. Permeabilized $Bak^{-/-}Bax^{-/-}$ MEFS expressing the indicated chimeras were incubated with tBid, and the cytosol and membrane fractions immunoblotted for Bak. (**d**) The Fis1 C terminus can be linked after BakFis1 forms an apoptotic pore. Membrane fractions from $Bak^{-/-}Bax^{-/-}$ MEFS expressing the indicated chimeras were incubated without or with tBid. Aliquots were assessed for linkage by CuPhe as in Figure 3a, or for cytochrome *c* release

helices became inserted as shown for peripherally attached Bax[34,48] and a semi-cytosolic Bak.[33] Insertion may be driven by activators binding the hydrophobic groove and releasing α9, but may be promoted by the membrane disturbance caused by collapse of activated Bak onto the MOM.[23] Somewhat surprisingly, Bak targeting and insertion could be severely affected by swapping the whole C terminus with that from other MOM tail-anchored proteins.

The Bak α9 TMD may not contribute directly to the pore structure. As protein pores and ion channels often have α-helices facing the pore lumen,[62,63] the same may be the case for pores formed by Bak and Bax. Although the Bax α5 and α6 helices were thought to insert into and traverse the membrane after Bax activation,[20] recent evidence that these helices in activated Bak and Bax lie in-plane on the membrane surface[22,23] leaves α9 as the only region likely to traverse the MOM either before or after apoptosis. Despite this, we found that Bak α9 did not line a pore, as IASD labeling did not increase along one side of the helix that

would become accessible to IASD present within the pore lumen. Single amphipathic helices such as melittin can form relatively stable 'lipidic' pores,[64] and hydrophobic peptides based on Bak or Bax α9 can also permeabilize mitochondria (Supplementary Figures S5a and b)[65] and vesicles.[41,43,46,47] However, green fluorescent protein (GFP) fused to Bax or Bak α9 was not reported to kill cells,[28,32,34,66] and we know of no instance in which a C-terminal transmembrane anchor in a full-length protein takes part directly in forming the pore. We note also that a Bak C terminus is not essential for the step of pore formation, as recombinant Bak with a hexahistidine tag in lieu of its C terminus can bind and permeabilize nickel-incorporated liposomes.[22] In summary, direct contribution of the Bak C terminus to the pore structure is not yet apparent.

An α9:α9 'interface' forms in the Bak apoptotic pore and can link dimers to higher-order oligomers. An α9:α9 interface in Bak (and Bax) oligomers was demonstrated by linkage of the α9 helices after pore formation, consistent with very recent evidence of an α9:α9 interface in Bax oligomers,

based on Förster resonance energy transfer (FRET)[29] and crosslinking.[67] A distinct cysteine linkage pattern along $\alpha9$ was not due to a dimerization domain, but may be caused by a preferred packing surface between the helices and/or by limited rotation of $\alpha9$ within oligomers. Linkage at Bak $\alpha9$:$\alpha9$ could link BH3:groove dimers to the higher-order oligomers that are associated with pore formation.[26,27] The dimers can also be linked via cysteine residues placed in $\alpha6$,[18,24,25] and more recently in $\alpha3$ or $\alpha5$,[6,21] suggesting a variety of dimer arrangements in the high-order complexes.

The Bak $\alpha9$:$\alpha9$ interface was not sufficient for cytochrome *c* release, consistent with BH3:groove dimerization being required for apoptosis.[14] It remains possible, however, that the $\alpha9$:$\alpha9$ interface disturbs the MOM in the same way that Bak

$\alpha9$ peptides do when permeabilizing liposomes[41,42] or mitochondria (Supplementary Figure S5b), but that small aggregates are not sufficient for permeabilization. For example, the number of TMDs that can co-localize will be limited by other Bak regions lying on the membrane surface (Figure 7d). Attempts to block the Bak $\alpha9$:$\alpha9$ interface by expressing an mCherry–Bak$\alpha9$ fusion protein were not successful, although the fusion protein may not have co-localized with Bak either before or after apoptosis (Supplementary Figures S5c–e).

The $\alpha6$–$\alpha9$ region is flexible in the Bak pore. When Bak molecules were linked within the MOM bilayer ($\alpha9$:$\alpha9$) and on the cytosolic side (BH3:groove or $\alpha6$:$\alpha6$) or in the intermembrane space (C-segment:C-segment), higher-order complexes were observed in each case. This demonstrates not only that each of the 'interfaces' can be distinct, but that there is significant flexibility within this region. Thus, our data suggest that dimers of Bak may adopt the membrane topology illustrated in Figure 7d. For example, the $\alpha2$–$\alpha5$ core dimers of Bak (and of Bax) form a tight helical bundle in X-ray structures,[6,7] confirmed by $\sim100\%$ linkage at the BH3:groove interfaces in mitochondria experiments (e.g., Figure 3a).[14,18] Those core dimers lie in-plane on the MOM surface, as suggested by hydrophobic residues on the bent planar surface of the structures,[6,7] and more recently by IASD labeling of oligomeric Bak and oligomeric Bax in mitochondria experiments.[23] The $\alpha6$-helix also lies in-plane, however, in contrast to IASD labeling of the BH3:groove interface, IASD could label all tested $\alpha6$ residues except for those embedded in the MOM,[23] indicating that $\alpha6$ does not engage in tight protein–protein interactions. Between $\alpha5$ and $\alpha9$, four loops potentially allow multiple conformations of $\alpha6$–$\alpha9$. In our experiments, flexibility of the $\alpha6$–$\alpha9$ region would allow
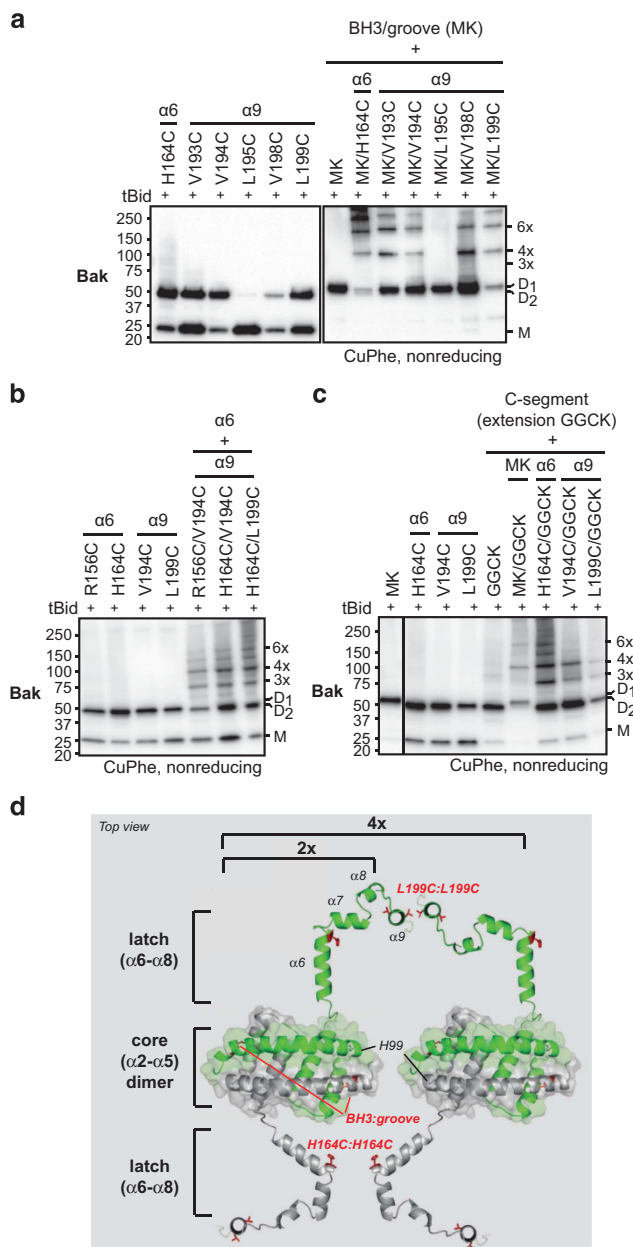

Figure 7 The $\alpha9$:$\alpha9$ interface can be linked independently of other interfaces, indicating a flexible $\alpha6$–$\alpha9$ region in oligomerized Bak. (**a**) Linkage at both the BH3:groove and $\alpha9$:$\alpha9$ interfaces generates high-order oligomers. Membranes expressing Bak with one, two or three cysteine residues as indicated, were incubated without or with tBid prior to treatment with CuPhe. Samples were analyzed as in Figure 3a. Note that linkage at the BH3:groove interface was tested using the M71C/K113C (MK) variant, and that this dimer (D$_1$) runs slightly higher than dimers linked elsewhere (D$_2$, see **d** below). Also note that trimers are absent due to complete linkage at the BH3:groove interface (for further details see Dewson *et al.*[24]). Data are representative of at least three independent experiments. (**b**) Linkage at both the $\alpha6$:$\alpha6$ and $\alpha9$:$\alpha9$ interfaces generates high-order oligomers. Note that trimers are observed because linkage at both $\alpha6$:$\alpha6$ or $\alpha9$:$\alpha9$ is incomplete (lanes 1–4). Samples were analyzed as in **a**. (**c**) Linkage at both the C-segment interface and $\alpha9$:$\alpha9$ interfaces generates high-order oligomers. Note that trimers are observed because linkage at both the C-segment interface and $\alpha9$:$\alpha9$ interfaces is incomplete (lanes 2–5). Samples were analyzed as in **a**. (**d**) Model of Bak dimers on the MOM surface illustrating the $\alpha9$:$\alpha9$ interface and the flexible $\alpha6$–$\alpha9$ region. Ribbon diagrams of the $\alpha2$–$\alpha5$ core dimer (4U2V),[6] the $\alpha6$–$\alpha8$ latch (from nonactivated Bak structure (2IMT),[4] and the Bak C terminus (see Figure 2c) were assembled and placed on the MOM surface. The in-plane positions of the $\alpha2$–$\alpha5$ core and $\alpha6$ are based on recent biochemical and structural studies.[6,21,23] The $\alpha9$ helix is seen end-on. Monomers of Bak $\alpha2$–$\alpha9$ are colored differently (green or gray) and certain linkages tested in **a**, **b** and **c** are shown as side chains (red). The N terminus ($\alpha1$ helix and $\alpha1$–$\alpha2$ loop) is not included. The flexible $\alpha6$–$\alpha9$ region is indicated by the ability of $\alpha6$:$\alpha6$ linkage (e.g., H164C:H164C) and $\alpha9$:$\alpha9$ linkage (L199C:L199C) to link between $\alpha2$–$\alpha5$ core dimers. The $\alpha2$–$\alpha5$ core dimers can also link via H99C:H99C,[6] suggesting their end-to-end arrangement may occur in oligomers

cysteine residues introduced in this region to come into close proximity, and be linked by CuPhe-induced disulfide bonds.

It remains unclear how dimers are arranged in high-order oligomers. The end-to-end arrangement of the dimerized $\alpha 2$–$\alpha 5$ core depicted in Figure 7d is consistent with linkage between either the $\alpha 3$ or $\alpha 5$ helices,[6,21] but there may be several arrangements that may change as membrane disturbance progresses to pore formation and even beyond. Which (if any) of the reported 'interfaces' is required for the high-order oligomerization and pore formation also remains unclear.

Our findings are consistent with aspects of two very recent studies of Bax oligomerization, as both reported an $\alpha 9$:$\alpha 9$ interface in addition to an interface involving the BH3 domains ($\alpha 2$).[29,67] Furthermore, the $\alpha 6$–$\alpha 9$ region in oligomerized Bax was found to be extended[29] and flexible.[67] Notably, Bleicken *et al.*[67] suggested the $\alpha 9$:$\alpha 9$ interaction 'within' dimers may be anti-parallel based on a model in which the $\alpha 2$–$\alpha 5$ core dimers position on the rim of the pore rather than facing the cytosol. Although our linkage studies and the FRET studies of Gahl *et al.*[29] show parallel interaction of the $\alpha 9$ helices, we may be detecting interactions 'between' dimers (as depicted in Figure 7d) and not the interactions that might occur 'within' dimers.

In conclusion, flexibility of the $\alpha 6$–$\alpha 9$ region suggests that the arrangement of the $\alpha 2$–$\alpha 5$ core dimers, for example, by lining a pore or aggregating on the surface or both, will be key to how Bak and Bax destabilize the MOM to generate pores.

Materials and Methods

Bak constructs, retroviral infection and cell culture. To generate mutations in Bak, BaxS184L and Bax, PCR mutagenesis (primer sequences available on request) was performed on Cys-null Bak, BaxS184L or Bax and cloned into the pMX (internal ribosome entry site (IRES))-GFP retroviral vector, as described previously.[14] The constructs were retrovirally expressed in SV-40-transformed $Bak^{-/-}Bax^{-/-}$ MEFs, and polyclonal populations of GFP-positive cells selected and cultured, as previously described.[14]

To generate the TMD chimeras, DNA for each Bak construct was chemically synthesized (Life Technologies GeneArt Gene Synthesis, Carlsbad, CA, USA). In the case of BakBcl2, a native cysteine in the C terminus was also replaced with serine. Synthesized DNA was then cloned into the pMX–IRES–GFP construct for retroviral expression in cells.

Apoptotic activation of Bak and Bax in cells and in mitochondrial membrane fractions. To activate Bak or Bax in cells, MEFs were treated with etoposide (10 μM) for 24 h and cell death determined by uptake of propidium iodide (5 μg/ml) using flow cytometry (FACScan or FACSCalibur, BD Biosciences, San Jose, CA, USA). To activate Bak or BaxS184L in mitochondrial assays, mitochondria-enriched membrane fractions were first obtained by resuspending MEFs at 1×10^7 cells/ml in permeabilization buffer (20 mM HEPES/KOH pH 7.5, 100 mM sucrose, 2.5 mM MgCl$_2$, 100 mM KCl, 0.025% digitonin and Complete protease inhibitors (Roche, Castle Hill, NSW, Australia)) and incubating on ice for 10 min. Membrane permeabilization was verified by uptake of trypan blue and cells were spun at 13 000 × g for 5 min. The resulting membrane fractions, with or without cytosol fractions as indicated, were then incubated with thrombin-cleaved Bid (tBid, 100 nM) for 30 min at 30 °C, as described previously.[14] To measure cytochrome *c* release, samples were centrifuged at 13 000 × g for 5 min and the supernatant (S/N) and pellet fractions were analyzed by immunoblotting.

IASD labeling and isoelectric focusing. To test whether each cysteine residue substituted in the Bak C termini was in a hydrophobic environment, membrane fractions were incubated with 10 mM IASD (Molecular Probes, Life Technologies), as described previously.[23] The 'before', 'during' and 'after' tBid incubations were conducted for 60 min each at 30 °C, with IASD added at 30 min.

The 'during tBid' samples had tBid also added at 30 min, whereas the 'after tBid' samples had tBid added at 0 min. In the 'denatured' samples, untreated membrane fractions were solubilized with 1% ASB-16 (w/v) for 10 min at RT prior to IASD labeling. Labeling was quenched by adding 200 mM dithiothreitol and samples solubilized with 1% ASB-16 (w/v; Calbiochem, Billerica, MA, USA) for 10 min at RT. After centrifugation at 13 000 × g for 5 min, the S/N was combined with an equal volume of isoelectric focusing (IEF) sample buffer (7 M urea, 2 M thiourea, 2% CHAPS, Complete protease inhibitors, 4 μg/ml pepstatin A, 1% ASB-16 and 0.04% bromophenol blue) and loaded immediately onto Novex pH 3-7 IEF gels (Life Technologies). Gels were focused with increasing voltage (100 V for 1 h, 200 V for 1 h, 500 V for 30 min) powered by the Consort EV265 power pack (Consort, Turnhout, Belgium). Gels were then soaked for 5 min in SDS buffer (75 mM Tris/HCl, pH 6.8, 0.6% SDS, 15% glycerol) and transferred at 40 mA for 2.5 h to PVDF membranes, and immunoblotted as for SDS-polyacrylamide electrophoresis (PAGE).

Bak subcellular localization and membrane insertion. Bak subcellular localization was assessed as described previously.[14] Briefly, MEFs were washed in ice-cold PBS and resuspended in permeabilization buffer. After incubation on ice for 10 min, cells were centrifuged at 13 000 × g for 5 min to separate cytosol and membrane fractions.

To assess Bak membrane insertion, membrane fractions were further resuspended in 0.1 M Na$_2$CO$_3$ (pH 11.5) and incubated on ice for 20 min. pH was neutralized with an equal volume of 0.1 M HCl and the sample incubated for 5 min before addition of 10 × nuclease buffer (400 mM Tris HCl, 100 mM MgSO$_4$, 10 mM CaCl$_2$) and 1 unit of DNAase I (Promega, Sydney, NSW, Australia), and incubation at 37 °C for a further 10 min. Samples were centrifuged at 13 000 × g for 10 min and S/N (peripheral) and pellet (inserted) fractions immunoblotted for Bak.

Immunoblotting. SDS-PAGE gels were transferred and immunoblotted for Bak using the rabbit polyclonal anti-Bak aa23–38 (Cat. #B5897, Sigma-Aldrich, Castle Hill, NSW, Australia). Other antibodies used were Rat monoclonal anti-Bax (Clone 49F9, generated in house by DCS Huang, WEHI, Parkville, VIC, Australia),[7] mouse monoclonal anti-cytochrome *c* (Clone 7H8.2C12; BD Biosciences Pharmingen, San Diego, CA, USA) and anti-HSP70 (Clone N6, gift from Drs R Anderson, Peter MacCallum Cancer Research Institute, Melbourne, VIC, Australia, and W Welch, University of California, San Francisco, CA, USA) antibodies. Horseradish peroxidase-conjugated anti-mouse (Cat. #1010-05, Southern Biotech, Birmingham, AL, USA), anti-rabbit (Cat. #4010-05, Southern Biotech) and anti-rat (Cat. #3010-05, Southern Biotech) IgG secondary antibodies were used. The proteins were detected using Luminata Forte western HRP substrate (WBLUF0500, Millipore, Billerica, MA, USA).

Cysteine linkage by disulfide bond formation or a chemical crosslinker. Cysteine linkage of Bak and BaxS184L in mitochondrial assays was assessed, as previously described.[14] Briefly, membrane fractions from digitonin-permeabilized MEFs were resuspended in crosslinking buffer (20 mM HEPES/KOH pH 7.5, 100 mM sucrose, 2.5 mM MgCl$_2$, 50 mM KCl) and incubated without or with 100 nM tBid for 30 min at 30 °C. To induce disulfide bonds, membrane fractions were removed from the 30 °C incubation to RT where the redox catalyst CuPhe was added to all samples, and the samples then moved to ice for 30 min.[14] The added CuPhe was a 100-fold dilution from a stock of 30 mM CuSO$_4$ and 100 mM 1,10-phenanthroline in 4 : 1 water/ethanol.[68] Oxidation by CuPhe was then quenched by adding 20 mM EDTA to chelate copper, and the samples analyzed by nonreducing SDS-PAGE and western blot. For chemical crosslinking of cysteine residues, membrane fractions were treated with the homobifunctional sulfhydryl-reactive crosslinker 1,6-bis-maleimidoethane (BMOE, 8 Å linker, Pierce, Thermo Fisher Scientific Inc., Rockford, IL, USA) at RT for 30 min. Crosslinking was quenched by addition of reducing sample buffer, and samples analyzed by reducing SDS-PAGE and western blot.

To assess Bax oligomerization in apoptotic cells, MEFs were treated with etoposide in the presence of the broad range caspase inhibitor Q-VD.oph (50 μM, Enzyme Systems, Livermore, CA, USA), followed by digitonin permeabilization. Cytosol and membrane fractions were separated by centrifugation at 13 000 × g for 5 min, and linkage performed as for BaxS184L.[18]

Conflict of Interest

The authors declare no conflict of interest.

1. Bender T, Martinou JC. Where killers meet–permeabilization of the outer mitochondrial membrane during apoptosis. *Cold Spring Harb Perspect Biol* 2013; **5**: a011106.
2. Tait SW, Green DR. Mitochondria and cell death: outer membrane permeabilization and beyond. *Nat Rev Mol Cell Biol* 2010; **11**: 621–632.
3. Westphal D, Dewson G, Czabotar PE, Kluck RM. Molecular biology of Bax and Bak activation and action. *Biochim Biophys Acta* 2011; **1813**: 521–531.
4. Moldoveanu T, Liu Q, Tocilj A, Watson MH, Shore G, Gehring K. The x-ray structure of a BAK homodimer reveals an inhibitory zinc binding site. *Mol Cell* 2006; **24**: 677–688.
5. Suzuki M, Youle RJ, Tjandra N. Structure of Bax: coregulation of dimer formation and intracellular localization. *Cell* 2000; **103**: 645–654.
6. Brouwer JM, Westphal D, Dewson G, Robin AY, Uren RT, Bartolo R *et al.* Bak core and latch domains separate during activation, and freed core domains form symmetric homodimers. *Mol Cell* 2014; **55**: 938–946.
7. Czabotar PE, Westphal D, Dewson G, Ma S, Hockings C, Fairlie WD *et al.* Bax crystal structures reveal how BH3 domains activate bax and nucleate its oligomerization to induce apoptosis. *Cell* 2013; **152**: 519–531.
8. Dai H, Smith A, Meng XW, Schneider PA, Pang YP, Kaufmann SH. Transient binding of an activator BH3 domain to the Bak BH3-binding groove initiates Bak oligomerization. *J Cell Biol* 2011; **194**: 39–48.
9. Du H, Wolf J, Schafer B, Moldoveanu T, Chipuk JE, Kuwana T. BH3 domains other than Bim and Bid can directly activate Bax/Bak. *J Biol Chem* 2011; **286**: 491–501.
10. Leshchiner ES, Braun CR, Bird GH, Walensky LD. Direct activation of full-length proapoptotic BAK. *Proc Natl Acad Sci USA* 2013; **110**: E986–E995.
11. Letai A, Bassik MC, Walensky LD, Sorcinelli MD, Weiler S, Korsmeyer SJ. Distinct BH3 domains either sensitize or activate mitochondrial apoptosis, serving as prototype cancer therapeutics. *Cancer Cell* 2002; **2**: 183–192.
12. Moldoveanu T, Grace CR, Llambi F, Nourse A, Fitzgerald P, Gehring K *et al.* BID-induced structural changes in BAK promote apoptosis. *Nat Struct Mol Biol* 2013; **20**: 589–597.
13. Gavathiotis E, Suzuki M, Davis ML, Pitter K, Bird GH, Katz SG *et al.* BAX activation is initiated at a novel interaction site. *Nature* 2008; **455**: 1076–1081.
14. Dewson G, Kratina T, Sim HW, Puthalakath H, Adams JM, Colman PM *et al.* To trigger apoptosis Bak exposes its BH3 domain and homo-dimerizes via BH3:grooove interactions. *Mol Cell* 2008; **30**: 369–380.
15. Griffiths GJ, Corfe BM, Savory P, Leech S, Esposti MD, Hickman JA *et al.* Cellular damage signals promote sequential changes at the N-terminus and BH-1 domain of the pro-apoptotic protein Bak. *Oncogene* 2001; **20**: 7668–7676.
16. Hsu YT, Youle RJ. Nonionic detergents induce dimerization among members of the Bcl-2 family. *J Biol Chem* 1997; **272**: 13829–13834.
17. Bleicken S, Classen M, Padmavathi PV, Ishikawa T, Zeth K, Steinhoff HJ *et al.* Molecular details of Bax activation, oligomerization, and membrane insertion. *J Biol Chem* 2010; **285**: 6636–6647.
18. Dewson G, Ma S, Frederick P, Hockings C, Tan I, Kratina T *et al.* Bax dimerizes via a symmetric BH3:groove interface during apoptosis. *Cell Death Differ* 2012; **19**: 661–670.
19. Chi X, Kale J, Leber B, Andrews DW. Regulating cell death at, on, and in membranes. *Biochim Biophys Acta* 2014; **1843**: 2100–2113.
20. Annis MG, Soucie EL, Dlugosz PJ, Cruz-Aguado JA, Penn LZ, Leber B *et al.* Bax forms multispanning monomers that oligomerize to permeabilize membranes during apoptosis. *EMBO J* 2005; **24**: 2096–2103.
21. Aluvila SM, Mandal T, Hustedt E, Fajer P, Choe JY, Oh KJ. Organization of the mitochondrial apoptotic BAK pore: oligomerization of the Bak homodimers. *J Biol Chem* 2014; **289**: 2537–2551.
22. Oh KJ, Singh P, Lee K, Foss K, Lee S, Park M *et al.* Conformational changes in BAK, a pore-forming proapoptotic Bcl-2 family member, upon membrane insertion and direct evidence for the existence of BH3-BH3 contact interface in BAK homo-oligomers. *J Biol Chem* 2010; **285**: 28924–28937.
23. Westphal D, Dewson G, Menard M, Frederick P, Iyer S, Bartolo R *et al.* Apoptotic pore formation is associated with in-plane insertion of Bak or Bax central helices into the mitochondrial outer membrane. *Proc Natl Acad Sci USA* 2014; **111**: E4076–E4085.
24. Dewson G, Kratina T, Czabotar P, Day CL, Adams JM, Kluck RM. Bak activation for apoptosis involves oligomerization of dimers via their alpha6 helices. *Mol Cell* 2009; **36**: 696–703.
25. Ma S, Hockings C, Anwari K, Kratina T, Fennell S, Lazarou M *et al.* Assembly of the Bak apoptotic pore: a critical role for the Bak protein alpha6 helix in the multimerization of homodimers during apoptosis. *J Biol Chem* 2013; **288**: 26027–26038.
26. Bleicken S, Landeta O, Landajuela A, Basanez G, Garcia-Saez AJ. Proapoptotic Bax and Bak proteins form stable protein-permeable pores of tunable size. *J Biol Chem* 2013; **288**: 33241–33252.
27. Korsmeyer SJ, Wei MC, Saito M, Weiler S, Oh KJ, Schlesinger PH. Pro-apoptotic cascade activates BID, which oligomerizes BAK or BAX into pores that result in the release of cytochrome *c*. *Cell Death Differ* 2000; **7**: 1166–1173.
28. Setoguchi K, Otera H, Mihara K. Cytosolic factor- and TOM-independent import of C-tail-anchored mitochondrial outer membrane proteins. *EMBO J* 2006; **25**: 5635–5647.
29. Gahl RF, He Y, Yu S, Tjandra N. Conformational rearrangements in the pro-apoptotic protein, Bax, as it inserts into mitochondria: a cellular death switch. *J Biol Chem* 2014; **289**: 32871–32882.
30. Edlich F, Banerjee S, Suzuki M, Cleland MM, Arnoult D, Wang C *et al.* Bcl-x(L) Retrotranslocates Bax from the mitochondria into the cytosol. *Cell* 2011; **145**: 104–116.
31. Wolter KG, Hsu YT, Smith CL, Nechushtan A, Xi XG, Youle RJ. Movement of Bax from the cytosol to mitochondria during apoptosis. *J Cell Biol* 1997; **139**: 1281–1292.
32. Nechushtan A, Smith CL, Hsu YT, Youle RJ. Conformation of the Bax C-terminus regulates subcellular location and cell death. *EMBO J* 1999; **18**: 2330–2341.
33. Ferrer PE, Frederick P, Gulbis JM, Dewson G, Kluck RM. Translocation of a Bak C-terminus mutant from cytosol to mitochondria to mediate cytochrome C release: implications for Bak and Bax apoptotic function. *PLoS One* 2012; **7**: e31510.
34. Schinzel A, Kaufmann T, Schuler M, Martinalbo J, Grubb D, Borner C. Conformational control of Bax localization and apoptotic activity by Pro168. *J Cell Biol* 2004; **164**: 1021–1032.
35. Cheng EH, Sheiko TV, Fisher JK, Craigen WJ, Korsmeyer SJ. VDAC2 inhibits BAK activation and mitochondrial apoptosis. *Science* 2003; **301**: 513–517.
36. Roy SS, Ehrlich AM, Craigen WJ, Hajnoczky G. VDAC2 is required for truncated BID-induced mitochondrial apoptosis by recruiting BAK to the mitochondria. *EMBO Rep* 2009; **10**: 1341–1347.
37. Lazarou M, Stojanovski D, Frazier AE, Kotevski A, Dewson G, Craigen WJ *et al.* Inhibition of Bak activation by VDAC2 is dependent on the Bak transmembrane anchor. *J Biol Chem* 2010; **285**: 36876–36883.
38. Ma SB, Nguyen TN, Tan I, Ninnis R, Iyer S, Stroud DA *et al.* Bax targets mitochondria by distinct mechanisms before or during apoptotic cell death: a requirement for VDAC2 or Bak for efficient Bax apoptotic function. *Cell Death Differ* 2014; **21**: 1925–1935.
39. Todt F, Cakir Z, Reichenbach F, Emschermann F, Lauterwasser J, Kaiser A *et al.* Differential retrotranslocation of mitochondrial Bax and Bak. *EMBO J* 2015; **34**: 67–80.
40. del Mar Martinez-Senac M, Corbalan-Garcia S, Gomez-Fernandez JC. Conformation of the C-terminal domain of the pro-apoptotic protein Bax and mutants and its interaction with membranes. *Biochemistry* 2001; **40**: 9983–9992.
41. Martinez-Senac M, Corbalan-Garcia S, Gomez-Fernandez JC. The structure of the C-terminal domain of the pro-apoptotic protein Bak and its interaction with model membranes. *Biophys J* 2002; **82**: 233–243.
42. Torrecillas A, Martinez-Senac MM, Goormaghtigh E, de Godos A, Corbalan-Garcia S, Gomez-Fernandez JC. Modulation of the membrane orientation and secondary structure of the C-terminal domains of Bak and Bcl-2 by lipids. *Biochemistry* 2005; **44**: 10796–10809.
43. Tatulian SA, Garg P, Nemec KN, Chen B, Khaled AR. Molecular basis for membrane pore formation by Bax protein carboxyl terminus. *Biochemistry* 2012; **51**: 9406–9419.
44. Ausili A, Torrecillas A, Martinez-Senac MM, Corbalan-Garcia S, Gomez-Fernandez JC. The interaction of the Bax C-terminal domain with negatively charged lipids modifies the secondary structure and changes its way of insertion into membranes. *J Struct Biol* 2008; **164**: 146–152.
45. Ausili A, de Godos A, Torrecillas A, Corbalan-Garcia S, Gomez-Fernandez JC. The interaction of the Bax C-terminal domain with membranes is influenced by the presence of negatively charged phospholipids. *Biochim Biophys Acta* 2009; **1788**: 1924–1932.
46. Torrecillas A, Martinez-Senac MM, Ausili A, Corbalan-Garcia S, Gomez-Fernandez JC. Interaction of the C-terminal domain of Bcl-2 family proteins with model membranes. *Biochim Biophys Acta* 2007; **1768**: 2931–2939.
47. Garg P, Nemec KN, Khaled AR, Tatulian SA. Transmembrane pore formation by the carboxyl terminus of Bax protein. *Biochim Biophys Acta* 2013; **1828**: 732–742.
48. Goping IS, Gross A, Lavoie JN, Nguyen M, Jemmerson R, Roth K *et al.* Regulated targeting of BAX to mitochondria. *J Cell Biol* 1998; **143**: 207–215.
49. Tran VH, Bartolo R, Westphal D, Alsop A, Dewson G, Kluck RM. Bak apoptotic function is not directly regulated by phosphorylation. *Cell Death Dis* 2013; **4**: e452.
50. Kim PK, Annis MG, Dlugosz PJ, Leber B, Andrews DW. During apoptosis bcl-2 changes membrane topology at both the endoplasmic reticulum and mitochondria. *Mol Cell* 2004; **14**: 523–529.
51. Colombini M, Mannella CA. VDAC, the early days. *Biochim Biophys Acta* 2012; **1818**: 1438–1443.
52. Bass RB, Butler SL, Chervitz SA, Gloor SL, Falke JJ. Use of site-directed cysteine and disulfide chemistry to probe protein structure and dynamics: applications to soluble and transmembrane receptors of bacterial chemotaxis. *Methods Enzymol* 2007; **423**: 25–51.
53. Fletcher JI, Meusburger S, Hawkins CJ, Riglar DT, Lee EF, Fairlie WD *et al.* Apoptosis is triggered when prosurvival Bcl-2 proteins cannot restrain Bax. *Proc Natl Acad Sci USA* 2008; **105**: 18081–18087.
54. Wattenberg. An artificial mtochondrial tail signal/anchor sequence confirms a requirement for moderate hydrophobicity for targeting. *Biosci Rep* 2007; **27**: 385–401.

55. Kaufmann T, Schlipf S, Sanz J, Neubert K, Stein R, Borner C. Characterization of the signal that directs Bcl-x$_L$, but not Bcl-2, to the mitochondrial outer membrane. *J Cell Biol* 2003; **160**: 53–64.

56. Lemmon MA, Flanagan JM, Hunt JF, Adair BD, Bormann BJ, Dempsey CE *et al*. Glycophorin A dimerization is driven by specific interactions between transmembrane alpha-helices. *J Biol Chem* 1992; **267**: 7683–7689.

57. Sulistijo ES, Mackenzie KR. Structural basis for dimerization of the BNIP3 transmembrane domain. *Biochemistry* 2009; **48**: 5106–5120.

58. Boohaker RJ, Zhang G, Lee MW, Nemec KN, Santra S, Perez JM *et al*. Rational development of a cytotoxic peptide to trigger cell death. *Mol Pharm* 2012; **9**: 2080–2093.

59. Ma J, Yoshimura M, Yamashita E, Nakagawa A, Ito A, Tsukihara T. Structure of rat monoamine oxidase A and its specific recognitions for substrates and inhibitors. *J Mol Biol* 2004; **338**: 103–114.

60. Mineev KS, Bocharov EV, Volynsky PE, Goncharuk MV, Tkach EN, Ermolyuk YS *et al*. Dimeric structure of the transmembrane domain of glycophorin a in lipidic and detergent environments. *Acta Naturae* 2011; **3**: 90–98.

61. Suzuki M, Jeong SY, Karbowski M, Youle RJ, Tjandra N. The solution structure of human mitochondria fission protein Fis1 reveals a novel TPR-like helix bundle. *J Mol Biol* 2003; **334**: 445–458.

62. Bocquet N, Nury H, Baaden M, Le Poupon C, Changeux JP, Delarue M *et al*. X-ray structure of a pentameric ligand-gated ion channel in an apparently open conformation. *Nature* 2009; **457**: 111–114.

63. Mueller M, Grauschopf U, Maier T, Glockshuber R, Ban N. The structure of a cytolytic alpha-helical toxin pore reveals its assembly mechanism. *Nature* 2009; **459**: 726–730.

64. Lee MT, Sun TL, Hung WC, Huang HW. Process of inducing pores in membranes by melittin. *Proc Natl Acad Sci USA* 2013; **110**: 14243–14248.

65. Valero JG, Cornut-Thibaut A, Juge R, Debaud AL, Gimenez D, Gillet G *et al*. micro-Calpain conversion of antiapoptotic Bfl-1 (BCL2A1) into a prodeath factor reveals two distinct alpha-helices inducing mitochondria-mediated apoptosis. *PLoS One* 2012; **7**: e38620.

66. Valero JG, Sancey L, Kucharczak J, Guillemin Y, Gimenez D, Prudent J *et al*. Bax-derived membrane-active peptides act as potent and direct inducers of apoptosis in cancer cells. *J Cell Sci* 2011; **124**: 556–564.

67. Bleicken S, Jeschke G, Stegmueller C, Salvador-Gallego R, Garcia-Saez AJ, Bordignon E. Structural model of active bax at the membrane. *Mol Cell* 2014; **56**: 496–505.

68. Careaga CL, Falke JJ. Thermal motions of surface alpha-helices in the D-galactose chemosensory receptor. Detection by disulfide trapping. *J Mol Biol* 1992; **226**: 1219–1235.

69. Cole C, Barber JD, Barton GJ. The Jpred 3 secondary structure prediction server. *Nucleic Acids Res* 2008; **36**: W197–W201.

70. Tripos Inc. SYBYL-X 1.2, Tripos International, St. Louis, MO, USA. 2005. http://www.certara.com.

71. Grundling A, Blasi U, Young R. Biochemical and genetic evidence for three transmembrane domains in the class I holin, lambda S. *J Biol Chem* 2000; **275**: 769–776.

72. Riek RP, Rigoutsos I, Novotny J, Graham RM. Non-alpha-helical elements modulate polytopic membrane protein architecture. *J Mol Biol* 2001; **306**: 349–362.

Supplementary Information accompanies this paper on Cell Death and Differentiation website (http://www.nature.com/cdd)